# Polymer Chemistry



PAPER View Article Online
View Journal | View Issue



**Cite this:** *Polym. Chem.*, 2021, **12**, 5831

Design, synthesis, and characterization of vinyladdition polynorbornenes with tunable thermal properties†

Xinyi Wang,<sup>a</sup> Yewon L. Jeong,<sup>b</sup> Christopher Love,<sup>a</sup> Holly A. Stretz, <sup>©</sup> Gila E. Stein <sup>©</sup> \* and Brian K. Long <sup>©</sup> \* a

Unfunctionalized vinyl-addition polynorbornene (VAPNB) possesses many outstanding properties such as high thermal, chemical, and oxidative stability. These features make VAPNB a promising candidate for many engineering applications. However, VAPNB has a small service window between its glass transition temperature ( $T_{\rm g}$ ) and decomposition temperature ( $T_{\rm d}$ ), and it cannot be readily processed in a melt state. In this work, we demonstrate that the service window of VAPNBs can be tailored through the use of norbornene monomers bearing alkyl, aryl, and aryl ether substituents. The vinyl addition homopolymerization and copolymerization of these functionalized norbornyl-based monomers yielded VAPNBs with high  $T_{\rm g}$ s (>150 °C) and large service windows ( $T_{\rm d}-T_{\rm g}$  > 100 °C), which are comparable to other commercial engineering thermoplastics. To further establish the feasibility of melt processing, a functionalized VAPNB material with  $T_{\rm g}$  = 209 °C and a service window of 170 °C was successfully extruded and molded into bars. Subsequent characterization of the bars by dynamic mechanical analysis (DMA), nuclear magnetic resonance spectroscopy (NMR), and gel permeation chromatography (GPC) revealed only minor signs of polymer degradation. These studies suggest that substituted VAPNBs could be developed into a new class of engineering thermoplastics that is compatible with workhorse melt processing techniques such as extrusion and injection molding, as well as emerging techniques such as extrusion-based 3D printing.

Received 5th August 2021, Accepted 21st September 2021 DOI: 10.1039/d1py01050f

rsc.li/polymers

## Introduction

Unfunctionalized vinyl-addition polynorbornene (VAPNB) possesses many outstanding properties, such as high thermal, chemical, and oxidative stability, as well as low birefringence, a low dielectric constant, and low moisture absorbance. These properties make VAPNB a promising candidate for many engineering and high-performance applications. However, unfunctionalized VAPNB has limited solubility in organic solvents, mechanical brittleness, and a small service window between its glass transition  $(T_{\rm g})$  and decomposition temperatures  $(T_{\rm d})$ , all of which limit its processability.

Several studies have shown that the homopolymerization and/ or copolymerization of norbornyl monomers bearing polar or nonpolar substituents can improve both polymer solubility and mechanical properties. Such functionalized VAPNBs can often be solution processed into mechanically robust, freestanding films that are suitable for a variety of potential applications, including gas separations, spervaporation membranes, in ion-exchange membranes, heproperation interconnects, and nonlinear-optical devices. In contrast, in the fields of extrusion, injection molding, film blowing, or 3D printing, where commercial thermoplastics are widely used, few comprehensive studies of improving VAPNB melt processability by employing substituted norbornene monomers exist in the peer-reviewed literature. 14,24

To facilitate the melt processing of VAPNBs, their glass transition temperature  $(T_{\rm g})$  must be lowered while maintaining a high decomposition temperature  $(T_{\rm d})$  to establish a broad service window and enable melt flow without decomposition. Indeed, prior reports have demonstrated that certain functionalized VAPNBs may exhibit depressed  $T_{\rm g}$ s while simultaneously maintaining high  $T_{\rm d}$ s,  $^{10,12-14,16,17,25}$  and companies such as BFGoodrich and Promerus have commercialized several VAPNB derivatives with  $T_{\rm g}$ s well below that of unsubsti-

<sup>&</sup>lt;sup>a</sup>Department of Chemistry, University of Tennessee, Knoxville, Tennessee, 37996-1660, USA. E-mail: blong20@utk.edu

<sup>&</sup>lt;sup>b</sup>Department of Chemical & Biomolecular Engineering, University of Tennessee, Knoxville, Tennessee, 37996-1660, USA. E-mail: gstein4@utk.edu

<sup>&</sup>lt;sup>c</sup>Department of Chemical Engineering, Tennessee Tech University, Cookeville, Tennessee, 38505, USA

<sup>†</sup> Electronic supplementary information (ESI) available: Tabulated thermal data; NMR spectra of monomer and polymers; GPC plots of polymers; TGA, DSC, spectroscopic ellipsometry, DMA traces; catalyst effect on polymer thermal properties; data comparing P2 before and after melt extrusion; and molecular weight influence on polymer thermal properties. See DOI: 10.1039/d1py01050f

Paper

tuted VAPNB. 2,3,6,26-29 As an example, Goodall and coworkers showed that copolymerization of alkyl-substituted norbornenes and unsubstituted norbornene could be used to finetune VAPNB  $T_{g_1}^{25}$  suggesting that melt processable VAPNBs may be accessed through careful substituent choice. This was also demonstrated by another recent report by Kim, Park, Huh and coworkers.<sup>14</sup> However, the overall relationships between thermal properties and molecular design are difficult to infer from current literature due to broad variability in the synthetic and thermal characterization methods used. 4,7,8,11,15,30,31 For example, polymer microstructure (i.e. stereoregularity, tacticity) may be strongly influenced by the type of catalyst used, and these attributes may impact resultant thermal properties. 1,2,32 Additional complications arise in that commonly employed techniques for characterization of  $T_g$ , such as differential scanning calorimetry (DSC),8 spectroscopic ellipsometry,33 and dynamic mechanical analysis (DMA), 12,13,15 often produce values that do not agree well with one another, particularly as each method probes a different property.

To provide fundamental insight into how monomer substituent structure may be used to tailor VAPNB  $T_g$  and service window  $(T_d - T_g)$ , we examined a systematic series of substituted VAPNB homopolymers and copolymers bearing polar and/or nonpolar functional groups. To ensure consistency and comparability of results, all polymers were synthesized using a single catalyst/activator system34 under identical reaction conditions. The  $T_{\rm d}$  of each polymer was measured by thermogravimetric analysis (TGA), and  $T_{\rm g}$  was measured using DMA. For a few selected polymers, these  $T_g$  values were then compared to those measured using DSC and spectroscopic ellipsometry. Copolymer  $T_g$  values were compared to predictions based on homopolymer values using either the Fox or Gordon-Taylor equations, providing insight into the predictive capability of these simple correlations when substituents differing in structure and intermolecular interactions (e.g., London dispersion forces,  $\pi$ - $\pi$  stacking, and dipole-dipole interactions) are introduced.

Though melt processing of VA-PNBs remains virtually unexplored in the peer-reviewed literature, recent work by Kim, Park, Huh and coworkers used melt pressing to prepare thin samples of unsubstituted-co-alkyl-substituted VAPNBs for tensile testing.<sup>14</sup> However, to the best of our knowledge, there are no literature examples in which melt extrudability is demonstrated. While a broad service window is required for thermal processing, this condition is not sufficient to establish processability by techniques such as melt extrusion. Therefore, to conclude our study, we selected a substituted VAPNB with a broad service window  $(T_{\rm d}$ – $T_{\rm g} \approx 200$  °C) for extrusion tests. We found that this substituted VAPNB exhibited melt processability similar to that of polystyrene (PS), and characterization of the extruded material by GPC, NMR spectroscopy, and DMA showed negligible signs of polymer degradation. These studies demonstrate that substituted VAPNBs may be engineered to enable their processing by workhorse techniques such as extrusion, thereby potentially broadening the application scope of this class of high-performing polyolefin-based materials.

## **Experimental section**

#### General materials and methods

All reactions were conducted under an inert atmosphere using an MBraun glovebox and a dry nitrogen atmosphere, unless noted otherwise. Synthesized monomers were purified via sequential distillations (≥98% purity, via GC) unless otherwise noted, degassed via freeze-pump-thaw (×3), and stored over 3 Å molecular sieves in a glovebox prior to use. Dicyclopentadiene, hydroquinone, 1-hexene, 1-octene, and sodium borohydride were purchased from Acros Organics and used as received. 1-Decene and 1-dodecene were purchased from TCI America and used as received. 5-Norbornene-2-carboxaldehyde and benzyl bromide were purchased from Alfa Aesar and used as received. Sodium hydride, allylmagnesium chloride solution (2.0 M in THF), and (2-bromoethyl)benzene were purchased from Sigma-Aldrich and used as received. Hexane, ethyl acetate, methanol, and chloroform were purchased from Fisher Scientific and used as received. Dichloromethane for polymerizations was purchased from Scientific and purified using an Innovative Technologies PureSolv Solvent Purification System and degassed via freeze-pump-thaw (×3) prior to use. The catalyst  $(\eta^3$ -allyl)Pd(i-Pr<sub>3</sub>P)Cl was synthesized according to literature procedure and stored in a glovebox prior to use. 34 This catalyst is commonly used for vinyl-addition polymerization of norbornene-based monomers. 11,15,17,31 Lithium tetrakis (pentafluorophenyl)borate ethyl etherate (LiBArF4) was obtained as a gift from Boulder Scientific and used as received. Monomers M1-M4 were synthesized according to prior literature reports with only minor modifications. 35,36 The intermediate 5-phenyl-1pentene,<sup>37</sup> 5-norbornene-2-methanol<sup>38</sup> and 5-benzyloxymethyl-2-norbornene (M6)<sup>38-40</sup> were synthesized according to prior literature reports and all characterization matched those previously reported. PS  $(M_{\rm w} \sim 350 \text{ kg mol}^{-1}, M_{\rm n} \sim 170 \text{ kg mol}^{-1})$ was purchased from Sigma Aldrich and used as a comparison sample for thermal characterization, melt processing, and mechanical characterization.

#### Synthesis of 5-butyl-2-norbornene (M1)

Monomer M1 was synthesized following a modified literature procedure. 35,36 1-Hexene (4.0 g, 47.5 mmol), dicyclopentadiene (2.5 g, 18.9 mmol), and hydroquinone were added to a 50 mL glass pressure tube with a stir bar. The pressure tube was sealed and heated to 240 °C for 3 h with stirring. After cooling, the mixture was purified by two sequential distillations at reduced pressure (10 torr, 88-90 °C) to yield 0.58 g of monomer M1 (10.3% yield) as a mixture of endo: exo isomers (endo: exo = 75:25). All characterizations matched prior literature reports.35

## Synthesis of 5-hexyl-2-norbornene (M2)

Monomer M2 was synthesized following the procedure described for M1. The crude mixture of M2 was purified by two sequential distillations at reduced pressure (4 torr, 113–115 °C) to yield 1.11 g of monomer **M2** (16.5% yield) as a

mixture of *endo*: exo isomers (endo: exo = 79:21). All characterizations matched prior literature reports.<sup>41</sup>

#### Synthesis of 5-octyl-2-norbornene (M3)

Monomer M3 was synthesized following the procedure described for M1. The crude mixture of M3 was purified by two sequential distillations at reduced pressure (4 torr, 132–134 °C) to yield 1.11 g of monomer M3 (17.0% yield) as a mixture of *endo*: *exo* isomers (*endo*: *exo* = 79:21). <sup>1</sup>H NMR (CDCl<sub>3</sub>, 293 K, *endo* isomer):  $\delta$  (ppm) = 6.10 (1H, dd), 5.91 (1H, dd), 2.75 (2H, m), 1.96 (1H, m), 1.83 (1H, m), 1.39 (1H, m), 1.35–1.22 (12H, m), 1.19 (1H, m), 1.07 (2H, m), 0.88 (3H, t), 0.48 (1H, ddd). <sup>13</sup>C NMR (CDCl<sub>3</sub>, 293 K, *endo/exo* mixture):  $\delta$  (ppm) = 137.16, 137.03, 136.36, 132.67, 49.78, 46.59, 45.64, 45.44, 42.75, 42.09, 39.00, 36.87, 35.06, 33.33, 32.68, 32.17, 30.19, 30.17, 29.92, 29.90, 29.59, 29.13, 28.91, 22.93, 14.35. HRMS<sup>calc</sup> C<sub>15</sub>H<sub>26</sub> (H<sup>+</sup> adduct) = 207.1858 *m/z*.

#### Synthesis of 5-decyl-2-norbornene (M4)

Monomer M4 was synthesized following the procedure described for M1. The crude mixture of M4 was purified by two sequential distillations at reduced pressure (0.5 torr, 110–112 °C) to yield 1.11 g of monomer M4 (12.1% yield) as a mixture of *endo*: *exo* isomers (*endo*: *exo* = 78:22). <sup>1</sup>H NMR (CDCl<sub>3</sub>, 293 K, *endo* isomer):  $\delta$  (ppm) = 6.10 (1H, dd), 5.91 (1H, dd), 2.75 (2H, m), 1.96 (1H, m), 1.83 (1H, m), 1.39 (1H, m), 1.35–1.22 (16H, m), 1.19 (1H, m), 1.07 (2H, m), 0.88 (3H, t), 0.48 (1H, ddd). <sup>13</sup>C NMR (CDCl<sub>3</sub>, 293 K, *endo/exo* mixture):  $\delta$  (ppm) = 137.16, 137.03, 136.36, 132.67, 49.78, 46.59, 45.64, 45.44, 42.75, 42.09, 39.00, 36.87, 35.07, 33.33, 32.68, 32.17, 30.19, 30.17, 29.96, 29.94, 29.90, 29.60, 29.14, 28.91, 22.93, 14.35. HRMS<sup>calc</sup> C<sub>17</sub>H<sub>30</sub> (H<sup>+</sup> adduct) = 235.2426 *m/z*. HRMS<sup>expt</sup> C<sub>17</sub>H<sub>30</sub> (H<sup>+</sup> adduct) = 235.2161 *m/z*.

## Synthesis of 5-phenylpropyl-2-norbornene (M5)

The reagent 5-phenyl-1-pentene was synthesized following a known literature procedure.<sup>37</sup> 5-Phenyl-1-pentene (5.84 g, 39.9 mmol), dicyclopentadiene (2.14 g, 16.2 mmol), and hydroquinone were added to a 50 mL glass pressure tube with a stir bar. The pressure tube was then sealed and heated to 240 °C for 12 h with stirring. The mixture was cooled to room temperature and purified by two sequential distillations at reduced pressure (0.5 torr, 130-132 °C) to yield 1.75 g of monomer M5 (25.4% yield) as a mixture of endo: exo isomers (endo: exo = 76:24). <sup>1</sup>H NMR (CDCl<sub>3</sub>, 293 K, endo isomer):  $\delta$  (ppm) = 7.31-7.17 (5H, m), 6.11 (1H, dd), 5.90 (1H, dd), 2.77 (2H, m), 2.58 (2H, m), 2.01 (1H, m), 1.84 (1H, m), 1.74-1.08 (6H, m), 0.50 (1H, ddd). <sup>13</sup>C NMR (CDCl<sub>3</sub>, 293 K, endo/exo mixture):  $\delta$  (ppm) = 143.12, 143.03, 137.16, 137.08, 136.40, 132.55, 128.55, 128.45, 128.42, 125.79, 125.76, 49.77, 46.56, 45.58, 45.45, 42.73, 42.09, 38.91, 38.86, 36.47, 36.43, 34.72, 33.26, 32.61, 30.98, 30.79. HRMS<sup>calc</sup>  $C_{16}H_{20}$  (H<sup>+</sup> adduct) = 213.1643 m/z. HRMS<sup>expt</sup>  $C_{16}H_{20}$  (H<sup>+</sup> adduct) =  $213.1407 \ m/z$ .

#### General polymerization procedure

Under air-free conditions (glovebox), ( $\eta^3$ -allyl)Pd(i-Pr<sub>3</sub>P)Cl (10 µmol), LiBAr<sup>F</sup><sub>4</sub> (10 µmol), and dry/degassed DCM (1 mL) were combined in a 20 mL scintillation vial and stirred for 20 min to activate the catalyst. In a separate vial, the monomer (or monomers) (5 mmol, total) was dissolved in dry/degassed DCM (4 mL) and added to the stirred catalyst solution. All polymerizations were ran overnight, unless otherwise noted, before quenching *via* exposure to air, dilution with additional DCM (10 mL), and precipitation into 250 mL of methanol. All polymers were isolated by vacuum filtration and dried *in vacuo* until reaching constant weight.

## Monomer and polymer characterization

 $^{1}$ H and  $^{13}$ C NMR spectra of monomers and polymers were obtained in CDCl $_{3}$  using a Varian 300 MHz or Varian 500 MHz NMR instrument, and spectra were referenced to the residual solvent peak at  $\delta$  = 7.26 ppm ( $^{1}$ H) and 77.23 ppm ( $^{13}$ C), respectively. High-resolution mass spectrometry (HRMS) was performed using a JEOL AccuTOF equipped with a DART source. Molecular weight and dispersity (D) of all polymers were determined using a Tosoh EcoSEC GPC with a refractive index detector and THF as the eluent at 40 °C. All MW's and dispersity values are reported relative to polystyrene standards.

## Thermal characterization of polymers

Thermogravimetric analysis (TGA) was performed using a TA Instruments Q550 with a heating rate of 10 °C min<sup>-1</sup> under a  $N_2$  purge. All  $T_d$  values are reported as the temperature corresponding to 5% weight loss. To measure  $T_g$ , three methods were employed: modulated DSC (MDSC), spectroscopic ellipsometry, and DMA. MDSC measurements were performed using compressed polymer powders in T-zero pans with a TA Instruments Q2000 at a heating rate of 3 °C per minute (modulated at ±1.00 °C per 60 s) from 80 to 300 °C under a nitrogen atmosphere.  $T_{\rm g}$  was determined based upon the transition of reversing heat capacity. DMA was performed using a TA Instruments RSA-G2 solids analyzer equipped with a tension fixture. Thick VAPNB film samples (40-120 µm) were prepared by solution casting from CHCl<sub>3</sub> solutions (3 wt%) into a PTFE dish. For example, a desired polymer (0.5 g) was added to CHCl<sub>3</sub> (10 mL) and stirred until fully dissolved. The solution was filtered through a 0.45 µm PTFE syringe filter into a clean and leveled PTFE dish that is approximately 6 cm in diameter. In contrast, polystyrene films were prepared by dissolving the commercial polystyrene sample (0.5 g) in toluene (3 mL), which was then filtered through a 0.45 µm PTFE syringe filter, degassed, and poured onto a levelled glass plate and drawn using a blade coater under a controlled shear rate. The solution cast VAPNB and drawn polystyrene films were covered to reduce the rate of evaporation while drying, and the polymer films were collected after complete solvent evaporation. Resultant films were determined to be 40–120 µm in thickness and were cut into strips (3-5 mm wide by 10-15 mm long) for DMA testing. The strips were mounted in the tension fixture,

equilibrated at the starting temperature for 5 min, and the experiment was run at a heating rate of 5 °C min<sup>-1</sup> from either 100 °C or 40 °C up to 300 °C under a nitrogen atmosphere with an axial force oscillated at 0.1% strain rate and 1 Hz. The  $T_{\rm g}$  was taken as the maximum of the tan  $\delta$  curve, and the reported value is the average of two measurements. Spectroscopic ellipsometry was used to measure thin film  $T'_{g}$ s. Films were prepared by spin casting from a toluene solution (~5 wt%) onto a silicon wafer and heated to 240 °C for 20 min under a nitrogen atmosphere to drive-off residual solvent. All films were 500 ± 50 nm in thickness. A J.A. Woollam M-2000 spectroscopic ellipsometer (wavelengths  $\lambda = 300-1690$  nm) was used to record the ellipsometry parameters  $\Delta$  and  $\psi$  as a function of temperature. The incidence/detection angles were fixed at 70°, and samples were heated/cooled at a rate of 1 °C min<sup>-1</sup> from 80 to 240 °C under a nitrogen atmosphere. The ellipsometry parameters were modeled using a three-layer system of polymer, native oxide, and silicon (in air). The refractive index of the polymer layer was described by the Cauchy dispersion relation,  $n(\lambda) = A + B/\lambda^2$ , and the refractive index of both native oxide and silicon were fixed to known literature values. The Cauchy constants (A and B) and polymer film thickness h were adjustable parameters for regression analysis. Typical values for A and B parameters were around 1.5 and 0.005-0.008, respectively. The  $T_{\sigma}$  was determined as the point of change in slope on a plot of polymer film thickness versus temperature<sup>42</sup>

## Melt extrusion and characterization of mechanical properties

glass regimes, as shown in Fig. S46-S51 in the ESI.†

using data from the second cooling cycle. The  $T_{\rm g}$  is taken as the intersection of the two lines that capture the rubber and

All polymer samples were dried in vacuo at 85 °C overnight prior to use. Tensile bars were prepared using a DSM Micro-5 twin screw compounder and benchtop injection molding machine, which was operated at a barrel temperature of 210 °C for commercial polystyrene samples and 250 °C for VAPNBs, a mold temperature of 100 °C under N2 purge, 90 rpm, a melt index of 10-12 g per 10 min, and a back force of ~1000-1500 N on the screws. As limited quantities of the synthesized VAPNB materials were available, relative to what was needed for melt processing, these process conditions were deemed best, but were not optimized. A portion of the synthesized VAPNB material was used for purging the extruder to ensure clean extrusion conditions, and bars were checked for clarity by visual inspection using a light box, indicating completeness of purge throughout the process. Mechanical testing was performed using an Instron load frame model 5948 (horizontal testing, 1 kN load cell) at a strain rate of 0.1 mm min<sup>-1</sup> according to ASTM D638. The modulus was obtained by plotting engineering/true stress verses corresponding strain. Cyclic loading moduli were obtained by testing two specimens, each with three cycles of load and unload between 110-360 N.

#### Wide angle X-Ray scattering

Select films (P3, P4) were illuminated at normal incidence (transmission through the film thickness) under ambient con-

ditions using A Xenocs GeniX 3D microfocus source with a copper target (wavelength  $\lambda = 0.154$  nm). The sample to detector distance was 0.045 m. A Pilatus3 R\_300 K detector (Dectris) was used with pixel size of 172  $\mu$ m  $\times$  172  $\mu$ m. The data acquisition time was 5 min. The two-dimensional images from each measurement were azimuthally-integrated to yield a one-dimensional scattering profile of intensity I (a.u.) versus scattering vector q (Å<sup>-1</sup>).

## Discussion

As a basis for the design of melt processable VAPNBs, we surveyed the thermal characteristics of commercially available engineering thermoplastics, such as polysulfone, polyetherimide, and polycarbonate. This analysis revealed that each material displayed a  $T_{\rm g} > 150~{\rm ^{\circ}C}$  and a  $T_{\rm d}$ – $T_{\rm g} > 100~{\rm ^{\circ}C}$ . In an effort to design VAPNBs that provide a similarly large service window, albeit while maintaining a high  $T_d$ , a variety of homopolymers and copolymers were synthesized using substituted norbornene monomers. Monomers M1-M4 (Fig. 1) bear linear alkyl substituents of varying length, whereas monomers M5 and M6 incorporate bulky aromatic groups that are tethered by an alkyl or ether linkage, respectively. In addition to differences in flexibility and size, these substituents introduce the possibility of different types of intermolecular forces being present. For example, monomers M1-M4 are believed to interact primarily via weak London-Dispersion forces, whereas monomers M5 and M6 introduce a bulky benzyl substituent that may participate in  $\pi$ - $\pi$  stacking interactions that have been reported to improve film formation. 12 Furthermore, monomer M6 also adds the potential to introduce dipoledipole interactions as a result of its ethereal moieties.

Monomers M1-M5 were synthesized *via* Diels-Alder reaction of *in situ* cracked dicyclopentadiene and a corresponding dieneophile that was either commercially available or was synthesized following established literature procedures.<sup>37</sup> Each monomer was isolated as a clear liquid following successive vacuum distillations at reduced pressure (10–25% yield) until reaching >98% purity, as determined *via* gas chromatography. As a note, monomer M3 could only be obtained in 85% purity

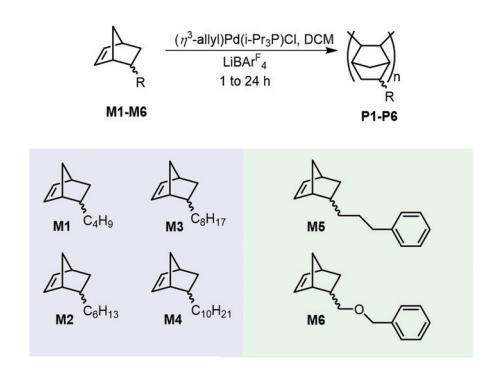


Fig. 1 Series of VAPNBs (P1–P6) chosen to probe the effects of substituent architecture on resultant thermal properties.

**Polymer Chemistry** Paper

due to the presence of impurities having similar boiling points that could not be readily removed via distillation or flash column chromatography. Monomer M6 was synthesized via Williamson ether synthesis in which 5-norbornene-2-methanol was reacted with benzyl bromide, followed by column chromatography to obtain a clear liquid (61% vield). Each monomer was characterized using 1H NMR spectroscopy to confirm functionalization and determine the endo: exo ratio of the norbornene substituent.

It is well known that the catalyst employed to access VAPNBs may influence the thermomechanical properties of the resultant materials, an effect that has been attributed to differences in polymer tacticity and stereoregularity. 25,43,44 We also observed this in our preliminary studies, wherein both Niand Pd-based catalysts were used (see ESI S47, S53, 54 and S65-67†). However, to avoid complications arising from tacticity and stereoregularity differences based upon catalyst choice, we chose to use the catalyst system (η³-allyl)Pd(i-Pr<sub>3</sub>P) Cl/LiBAr<sup>F</sup><sub>4</sub> (BAr<sup>F</sup><sub>4</sub> = tetrakis(pentafluorophenyl)-borate) for all polymer syntheses described herein. As shown in Fig. 1, monomers M1-M6 were each homopolymerized to yield polymers P1-P6. In order to further investigate the influence of various substituents on the thermal properties of VAPNBs, a series of statistical copolymers denoted using the notation PXPY were synthesized, wherein X and Y signify the two monomer components copolymerized. Specifically, X was fixed as M2 and Y was either M4, M5, or M6 to yield copolymers P2P4, P2P5, and P2P6, respectively.

Each polymer was obtained in modest to excellent yield (62–98%) and was characterized via <sup>1</sup>H NMR spectroscopy and gel permeation chromatography (GPC). All polymer molecular weights  $(M_n)$  exceeded 60 kg mol<sup>-1</sup> and dispersities (D) ranged from 1.3-2.8 (Table 1). It was noted that the homopolymerization of M3 resulted in higher molecular weight, higher dispersity and poorer solubility as compared to other VAPNB analogues. We hypothesize that this is due to the presence of impurities, such as tricyclopentadiene, that may have been incorporated into the polymer chain and could potentially lead to undesired crosslinking. Thus, a shorter reaction time (1 h) was applied to minimize the potential for crosslinking (Table 1, entry 3). In contrast, the homopolymerization of M6 (Table 1, entry 6) led to decreased polymer yield and molecular weight, even when polymerized at a higher monomer: catalyst ratio ([mon]:[cat] = 1000:1) and extended reaction time (24 h). Similar observations have been reported in the literature, in which slower polymerization rates and lower yields are often hypothesized to result from deleterious interactions between the polar substituent and the electrophilic, active catalyst species. 9,11,43,45 Similar trends were also found for all copolymerizations (Table 1, entries 13-15).

Copolymer compositions are denoted as PX<sup>n</sup>PY<sup>m</sup>, where the superscripts "n" and "m" represent the actual monomer incorporation ratios of each monomer (MX: MY). Monomer incorporation ratios for the **P2P4** copolymer series (entries 7–9) could not be determined by 1H NMR spectroscopy due to the significant overlap of all peaks in the alkyl region; however,

Table 1 Homo- and co-polymerization of substituted norbornene monomers

Entry	Polymer	Feed ratio (MX: MY)	Actual ratio $^d$ $(MX : MY)$	Yield (%)	$M_{\rm n}^f$ (kg mol <sup>-1</sup> )	$D^f$
1	P1	100:0	100:0	83	63	1.30
2	P2	100:0	100:0	85	84	1.35
$3^b$	P3	100:0	100:0	64	163	2.81
4	P4	100:0	100:0	92	129	2.00
5	P5	100:0	100:0	76	89	1.41
6 <sup>c</sup>	P6	100:0	100:0	62	66	1.32
7	$P2^{75}P4^{25}$	75:25	e	76	166	2.32
8	$P2^{50}P4^{50}$	50:50	e	97	159	2.20
9	$P2^{25}P4^{75}$	25:75	e	94	165	1.91
10	$P2^{68}P5^{32}$	75:25	68:32	96	92	1.47
11	$P2^{44}P5^{56}$	50:50	44:56	98	94	1.42
12	P2 <sup>15</sup> P5 <sup>85</sup>	25:75	15:85	97	94	1.46
13 <sup>c</sup>	P2 <sup>86</sup> P6 <sup>14</sup>	75:25	86:14	83	126	1.28
$14^c$	$P2^{65}P6^{35}$	50:50	65:35	75	102	1.29
$15^c$	P2 <sup>28</sup> P6 <sup>72</sup>	25:75	28:72	78	96	1.32

<sup>a</sup> General polymerization conditions: total monomer concentration = 5 mmol, [catalyst] = 10  $\mu$ mol, 5 mL of DCM, room temperature, and  $t_{\rm rxn}$  = 16 h. <sup>b</sup> Reaction time ( $t_{\rm rxn}$ ) = 1 h. <sup>c</sup> [mon]:[cat] = 1000:1 and  $t_{\rm rxn}$  = 24 h. <sup>d</sup> Monomer incorporation ratios (**MX:MY**) were calculated via <sup>1</sup>H NMR spectroscopy. <sup>e</sup>The monomer incorporation ratio (MX:MY) could not be determined via <sup>1</sup>H NMR spectroscopy due to overlapping <sup>1</sup>H resonances. <sup>f</sup>Molecular weights and dispersities were measured using gel permeation chromatography at 40 °C in THF and are reported relative to polystyrene standards.

the incorporation ratios for the copolymer series P2P5 and P2P6 (Table 1, entries 10-15) were readily determined based upon integration of their benzylic proton resonances corresponding to monomers M5 (2.59 ppm) and M6 (4.49 ppm), respectively, to all remaining protons in alkyl region. Therein, we found that copolymerizations of M2 and M5 favored higher incorporations of M5 than included in the feed, whereas copolymerizations of M2 and M6 favored higher incorporation of M2 than predicted based upon the monomer feed ratio. The lower observed incorporations of monomer M6 is consistent with the reduced polymerization rate often observed for monomers bearing polar substituents.46

As previously mentioned, VAPNB  $T_{\rm g}$  values can be probed via several techniques, such as DSC, DMA, and ellipsometry. 8,12,13,15,33 Unfortunately, each of these methods determines  $T_g$  by probing a different polymer property, resulting in data that may not be directly comparable to results obtained via another method. For example, DSC detects  $T_{\rm g}$ through changes in heat capacity above and below the glass transition, whereas DMA probes changes in viscoelastic properties (and depends on whether  $T_g$  was determined based upon storage modulus (E'), loss modulus (E''), or tan  $\delta$  peak), and ellipsometry detects  $T_{\rm g}$  through changes in the linear coefficient of thermal expansion.<sup>47</sup> We chose to evaluate all three techniques using a subset of the polymers described in Table 1 so as to compare each method of  $T_g$  determination. The polymers selected for this comparison were homopolymers P2, P6, the P2P6 copolymer series, and a PS control. Lastly, because the  $T_{\rm g}$  of each substituted VAPNB could not be detected using conventional DSC, MDSC was used for all studies described herein.  $^{48}$ 

As shown in Table 2, the  $T_g$  values obtained from MDSC, DMA, and spectroscopic ellipsometry for the PS control are similar, falling within 10 °C of each other. However, for VAPNB P2 and P6, a larger discrepancy (>30 °C) was observed. Similar results were found for the P2P6 copolymer series (range of 30-50 °C). Each method showed a similar trend in that increasing the molar ratio of M6 comonomer depressed the  $T_{g}$ , which was expected due to the increased flexibility of the ether linkage in monomer M6 as compared to alkyl-substituted M2. With the exception of entry 3,  $T_{\rm g}$  measurements obtained by MDSC and ellipsometry agree within 15 °C. This is consistent with a prior report that describes thermal characterization of VAPNB homopolymers, 33 and that can be attributed to the fact that heat capacity and thermal expansion coefficient are both thermodynamic properties. The discrepancy between these methods and DMA is likely explained by the fact that DMA does not probe a thermodynamic property, but

Table 2  $T_{\rm g}$  values of PS, P2, P6, and the P2P6 copolymer series as measured by MDSC, DMA, and ellipsometry

Entry	Polymer	$T_{\rm g}$ by MDSC (°C)	$T_{\rm g}$ by DMA (tan $\delta$ , °C)	$T_{\rm g}$ by ellipsometry <sup>a</sup> (°C)
1	PS	95 <sup>b</sup>	104	100
2	P2	189	209	173
3	P2 <sup>86</sup> P6 <sup>14</sup>	186	202	154
4	$P2^{65}P6^{35}$	162	191	160
5	$P2^{28}P6^{72}$	163	191	160
6	P6	162	184	152

 $<sup>^</sup>a$  Initial film thickness (h) was ~500 nm.  $^b$  The  $T_{\rm g}$  of PS was measured using conventional DSC.

rather employs both mechanical and thermal stimulation to measure a viscoelastic response. Ultimately, DMA was selected as the most useful method for characterizing the  $T_{\rm g}$  of the functionalized VAPNBs for a variety of reasons. First, the transitions obtained using MDSC and ellipsometry are extremely weak, and therefore difficult to detect and quantify with great accuracy (see ESI, Fig. S46–51†). In contrast, the  $\tan \delta$  peak obtained via DMA is strong and readily identifiable. Second, viscoelastic response is arguably more relevant to the design and tailoring of melt-processable polymers. Finally, the  $T_{\rm g}$  values obtained by DMA provide the most conservative estimate of the service window between  $T_{\rm g}$  and  $T_{\rm d}$ .

The  $T_{\rm g}$  (via DMA),  $T_{\rm d}$ , and service window of all the substituted VAPNB homopolymers are summarized in Fig. 2 and Table S1.† The  $T_{\rm g}$  and  $T_{\rm d}$  of unfunctionalized VAPNB are reported as approximately 390 °C and 415 °C, respectively. 3,32 The  $T_{\rm g}$ s of VAPNB homopolymers are significantly depressed by functionalization, which was expected due to the incorporation of flexible substituents.<sup>49</sup> Within the linear alkyl substituent series (P1-P4), the longer and more flexible substituents resulted in lower  $T_g$ s than their shorter analogues, with  $T_g$ decreasing from 280 °C for the butyl-substituted VAPNB (P1) to 119 °C for the decyl-substituted VAPNB (P4) (Fig. 2). As shown in Fig. S75,† WAXS measurements of P3 and P4 do not detect any crystallization of the long alkyl substituents. The addition of rigid and bulky phenyl substituents into polymer P5 introduces potential  $\pi$ - $\pi$  stacking interactions (P5) and was expected to increase the  $T_g$  relative to an alkyl substituent with the same number of carbons. Indeed, the  $T_{\rm g}$  of P5 which contains nine carbon atoms in its sidechain is similar to that of P3, which contains only 8 carbon atoms (Fig. 2). Furthermore, when ether linkages are introduced (P6), substituent flexibility is increased due to the lower rotational barrier of ethereal

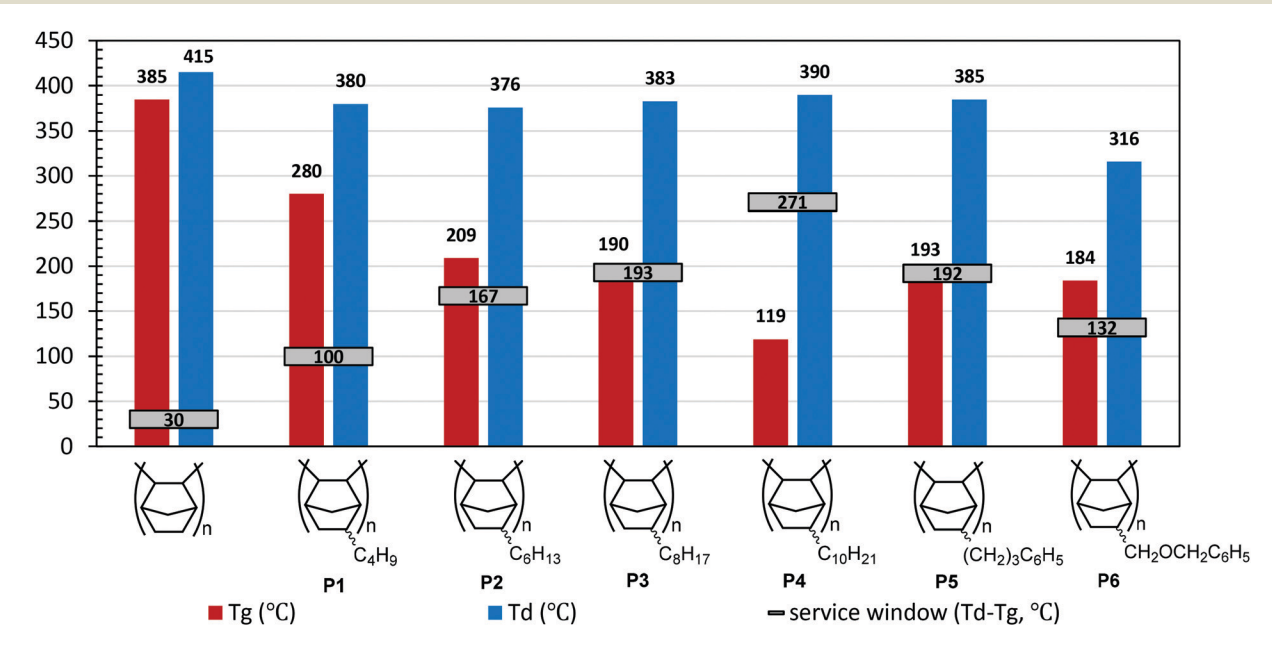


Fig. 2  $T_g$ ,  $T_d$ , and service window ( $T_d - T_g$ ) of unsubstituted VAPNB<sup>3,32</sup> and substituted homo-VAPNBs P1-P6

**Polymer Chemistry** 

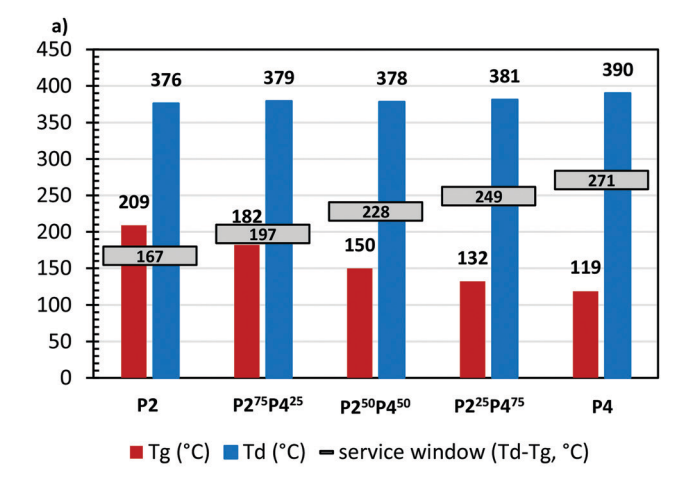
linkages as compared to analogous hydrocarbon linkers. This added flexibility results in  $T_{\rm g}$  being depressed from 193 °C for phenylpropyl-substituted P5 to 184 °C for benzyloxymethylsubstituted P6, despite having substituents of similar size and composition.

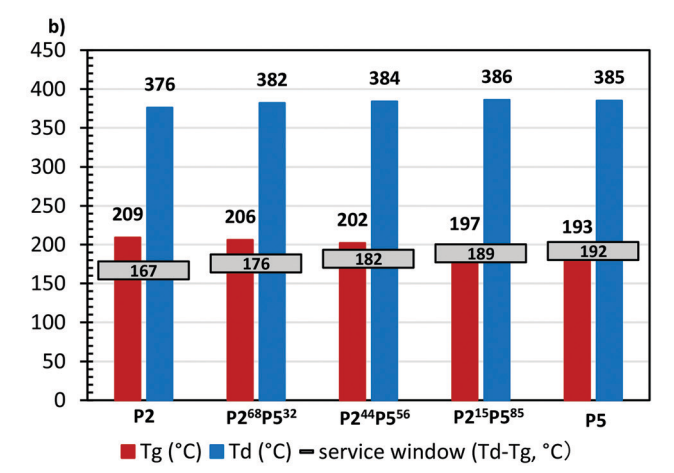
It should be noted that the  $T_{\rm g}$ s of the VAPNBs synthesized herein are generally lower than previously reported in the literature. Examples include P1 (280 °C) which has been previously reported to be 330 °C; 26 P2 (209 °C) which has been previously reported to be 265 °C, 3 280 °C, 13 or 225 °C; 26 and lastly, P4 (119 °C) which has been previously reported to be 150 °C, 13 or 180 °C. 26 As discussed previously, we hypothesize that this difference in measured  $T_g$  values may be attributed to the different catalysts and/or the characterization method being employed.

The  $T_{\rm d}$ s of VAPNB homopolymers are moderately depressed by functionalization, but aside from P6, all T<sub>d</sub>s exceeded ~380 °C. By inspecting the TGA data, the degradation behavior of P6 is different from P1-P5. Specifically, the derivative of the TGA curve of P6 suggests there are two stages of degradation, the first of which we hypothesize is degradation of the ether linkage prior to the second stage of backbone degradation (see ESI Fig. S36†). The key conclusion from the data in Fig. 2 and Table S1† is that functionalization more strongly depresses  $T_{\rm g}$ than  $T_{\rm d}$ , leading to a large service window for melt processing, while  $T_{\rm g}$  remains high enough to expect good thermomechanical stability. Furthermore, the  $T_g$ s and service windows of these VAPNB materials are comparable to those of commercial amorphous engineering thermoplastics, such as polycarbonate, and polyetherimide. 18,22,50

We also envisioned that the thermal properties of these VAPNB materials may be tuned via copolymerization, rather than relying solely on a single substituent chemistry. As an example, the  $T_{\rm d}$ s of P2 and P4 are both approximately 380 °C, yet the  $T_{\rm g}$ s of P2 and P4 are 209 °C and 120 °C, respectively. This suggests that copolymerization of M2 and M4 may enable tailoring of VAPNB  $T_{\rm g}$  across a broad 90 °C window with little impact on  $T_{\rm d}$ . As shown in Fig. 3 and Table S1,† the  $T_{\rm g}$ s of the P2P4 copolymer series fall within the anticipated range and provide potential melt processing temperature ranging from 150-350 °C. Similarly, the **P2P5** and **P2P6** copolymer series also demonstrates that  $T_{g}$ s can be designed to fall in between their homopolymer analogues, though admittedly this range is small due to the small difference in  $T_g$  values for homopolymers P2, P5, and P6. Aside from the P2P4 copolymer series that has high M4 comonomer content, the  $T_g$ s of these statistical copolymers fall within the range of 150-210 °C. Furthermore, the measured  $T_{\rm d}$  values for all copolymers exceeded ~380 °C, except the **P2P6** copolymer series which bears the M6 ether-containing monomer units (Fig. S43-45†). The service windows of these copolymers are comparable to those of commercial amorphous engineering thermoplastics as well.

To better understand the relationship between copolymer  $T_{\rm g}$ , comonomer composition, and potential intermolecular interactions present, we sought to compare our experimentally determined values to simple mathematical correlations.





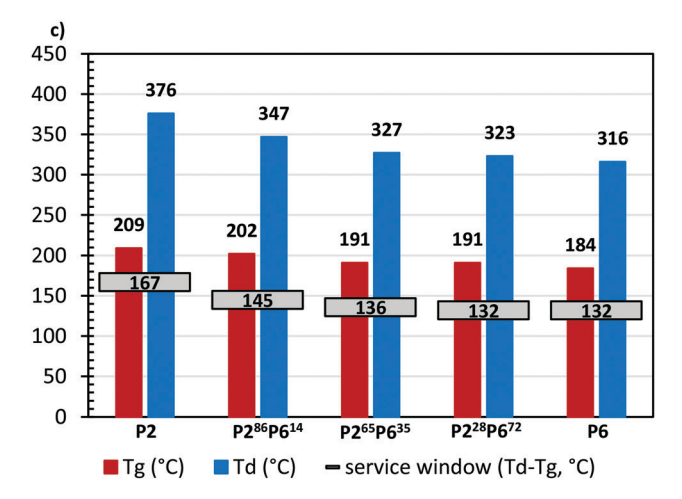


Fig. 3  $T_{\rm q}$ ,  $T_{\rm d}$ , and service window for the (a) P2P4, (b) P2P5, and (c) P2P6 copolymer series.

Starting with the alkyl substituted VAPNB copolymer series **P2P4**, theoretical copolymer  $T_g$ s were calculated using the Fox equation and compared to experimental  $T_{\rm g}$  data obtained via DMA (Fig. 4a). The Fox equation is as follows:

$$\frac{1}{T_{\rm g}} = \frac{w_1}{T_{\rm g1}} + \frac{1 - w_1}{T_{\rm g2}}$$

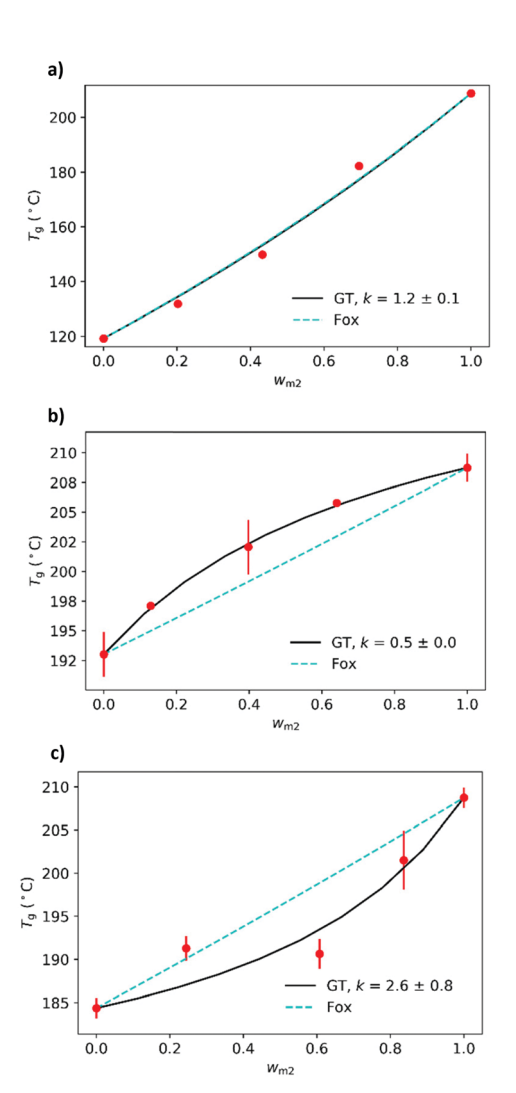


Fig. 4 Comparison of experimental  $T_{\rm g}$  (as determined by DMA) and theoretical  $T_q$  as predicted by the Fox and Gordon–Taylor equations for the (a) P2P4 series, (b) P2P5 series, and (c) P2P6 series.  $W_{\rm m2}$  is defined in each plot as the weight fraction of comonomer M2 in each copolymer. Error bars encompass the minimum and maximum values of two independent measurements. Note: in some series, the error bars are smaller than the symbol size.

where the parameters  $T_g$ ,  $w_1$ ,  $T_{g1}$ , and  $T_{g2}$  are the predicted glass transition temperature for the copolymer, the weight fraction of monomer type 1, and the measured glass transition temperatures of homopolymer types 1 and 2, respectively. The Fox equation provides excellent agreement with experimental data, confirming the validity of this simple model for alkyl substituted VAPNBs. Furthermore, there are no free parameters in this model, as  $T_{\rm g1}$  and  $T_{\rm g2}$  are measured from DMA. As a result, the  $T_{\rm g}$  and service window can be predicted as a function of  $w_1$  based solely on knowledge of the homopolymer  $T_{o}$ s.

In contrast to the simple alkyl substituted copolymer series P2P4, the P2P5 series mixes hexyl and phenylpropyl substituents, where the latter substituent has bulkier side chains that have the potential to introduce  $\pi$ - $\pi$  stacking interactions. As a result, chain packing in the solid state may be perturbed and

experimental  $T_g$  values may be observed that deviate from those predicted using the simple Fox equation. As shown in Fig. 4b, the **P2P5** copolymer series exhibits experimental  $T_{o}$ values that are larger than predicted using the simple Fox equation.

The P2P6 series combines hexyl and benzyloxymethyl substituents, where the latter introduces a rigid and bulky pendant group, increased linkage flexibility, the potential for  $\pi$ - $\pi$  stacking, and dipole-dipole interactions. As shown in Fig. 4c, this series displays negative deviations from the Fox equation. To better estimate the copolymer thermal properties, the Gordon-Taylor equation is used to capture deviations from ideal behavior:51,52

$$T_{\rm g} = \frac{w_1 T_{\rm g1} + k(1 - w_1) T_{\rm g2}}{w_1 + k(1 - w_1)}$$

The variable k is an adjustable fitting parameter. For P2P5 copolymer series, the trend is well-described with k = 0.5(Fig. 4b). Similarly, for P2P6 copolymer series, an optimized value of k = 2.6 provides qualitative agreement with the experimental trends (Fig. 4c).

While a broad service window is a requirement for melt processing, this criterion alone does not establish the suitability of a material for melt extrusion or injection molding. To demonstrate that substituted VAPNBs are indeed melt processable, homopolymer P2 was selected as a model and compared to commercially available PS. As a note, the entanglement molecular weight  $(M_e)$  of **P2** is estimated to be 33.1 kg mol<sup>-1</sup>, <sup>53</sup> and thus the samples synthesized herein  $(M_n = 163 \text{ kg mol}^{-1})$ are presumably entangled. As shown in Fig. 5, polymer P2  $(T_{\rm g}$  = 209 °C,  $T_{\rm d}$  = 376 °C) was readily melt processed into bars at 250 °C under a nitrogen atmosphere. The microcompounder in which the melt was formed (for subsequent injection molding) had a force plateau after 10 min of processing, which was used to compare relative melt viscosity of PS and P2 at low shear rate (90 rpm). In earlier work by Stretz and coworkers,<sup>54</sup> a PS (Styron 678 CW) sample reached 689 N of force when processed at 220 °C and 100 rpm; however, the commercial PS used in this study reached a force plateau of 1395 (±12) N (5





Fig. 5 Melt extruded bars of VAPNB P2. The dark color is presumed to be a consequence of residual catalyst decomposition/oxidation that occurs during melt processing.

replicates) at 210 °C and 90 rpm. This is remarkably similar to VAPNB **P2**, which reached a force plateau of 1483 (±32) N (3 replicates) at 250 °C and 90 rpm. This comparison shows that **P2** may be readily processed in similarity to some **PS** samples, needing only slightly elevated melt temperatures (250 °C) that are close to the commercial processing temperatures of many other engineering polymers (*e.g.*, nylon and polycarbonate).

Three additional qualitative processing observations were noted during melt extrusion. First, the extrudate was quite elastic, retracting a bit when cut. Second, the volume of the compounder (controlled by overflow at manufacturer specification of 5 cm3) was constant, and the average masses of PS and P2 melts were 2.43 g and 1.01 g, respectively. While these masses were recorded at different temperatures, the difference is larger than could be accounted for by temperature alone, suggesting that the P2 melt is a low-density material. This may be one possible reason for P2's surprisingly high degree of processibility compared to what might be expected for a rigid backbone polymer. Lastly, it was noted that the extruded specimens were dark in color, despite P2 being colorless prior to processing. We hypothesize that this color results due to residual catalyst decomposition and/or oxidation during processing.55 As a note, prior studies have shown that residual catalyst can be removed via a variety of methods, though this was not performed in this study. 14,30,55

The mechanical properties of the melt processed, **P2** bar specimens were then evaluated *via* tensile testing. As shown in Fig. 6, **P2** is softer (Young's modulus of 1291 MPa *vs.* 5765 MPa) and less brittle (0.01 mm mm<sup>-1</sup> *vs.* 0.0025 mm mm<sup>-1</sup> strain at yield) than **PS**. A cyclic loading test was also performed with **P2**, where the cyclic loading modulus is calculated to be 1349 MPa (Fig. S72†). While a complete study of substituted VAPNB mechanical properties is beyond the scope of this paper, these data demonstrate that melt processed VAPNBs have potential for real-world applications.

To determine the intactness of the processed polymer P2 after melt extrusion, thorough characterization of P2 was performed before and after extrusion, including NMR, GPC, and DMA (see ESI S68–S71†). <sup>1</sup>H NMR spectroscopy revealed that a minor set of new peaks (~5.3 ppm, Fig. S68†) were present in

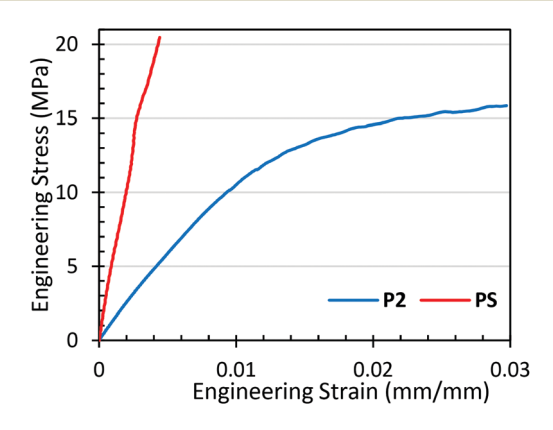


Fig. 6 Stress-strain curves for polymers P2 and PS.

the processed material that were not present prior to melting. We hypothesize that these resonances may result due to ring-opening of the bicyclic ring of VAPNB (around 3% of total, calculated by relative integration) to produce alkene containing polymers analogous to those of polynorbornene synthesized *via* ring-opening metathesis polymerization. This is supported by a recent report by Boydston and coworkers that demonstrates that many VAPNBs have intrinsic mechanochemical reactivity, producing partially ring-opened sequences along the main chain of VAPNBs when they are placed under mechanical activation (*e.g.* sonication). <sup>56</sup> We suspect that melt extrusion may act as a source of mechanical activation and lead to this conversion.

GPC characterization of melt processed P2 revealed that molecular weight decreased from  $M_n = 163$  to 117 kg mol<sup>-1</sup> following melt extrusion and exhibited a slightly increased dispersity (D = 1.83 vs. 1.60 for the original unprocessed sample) (Fig. S69†). This is consistent with previous reports in which polyolefins, such as polypropylene and polyethylene, undergo thermo-oxidative and/or thermo-mechanical induced chain scission.  $^{57}$  Additionally, **P2**'s average  $T_{\rm g}$  (from DMA) before and after melt extrusion was 209 °C and 205 °C, respectively. Though this observation is within one standard deviation of experimental results, the decreased  $T_g$  value is consistent with <sup>1</sup>H NMR spectroscopic analysis showing potential generation of ring-opened sequences along the main chain (Fig. S70†). Overall, it is concluded that the majority of the VAPNB P2 is intact after melt extrusion, but a small portion of the polymer may undergo chain scission due to oxidation and/or mechanical activation. DMA analysis also revealed that the extruded material's storage modulus (E') (at 100 °C) decreased slightly from E' = 0.49 GPa before melt extrusion to E' = 0.32 GPa after melt extrusion. In contrast, loss modulus (E'') before and after melt extrusion were similar at 0.031 GPa and 0.027 GPa, respectively (Fig. S71†).

## Conclusions

High molecular weight VAPNB homopolymers and copolymers bearing alkyl, aryl, and aryl ether functional groups were synthesized using a (η<sup>3</sup> – allyl)Pd(i-Pr<sub>3</sub>P)Cl/LiBAr<sup>F</sup><sub>4</sub> catalyst system. Each polymer's thermal characteristics ( $T_g$ ,  $T_d$ , and service window  $T_{\rm d}$ – $T_{\rm g}$ ) were evaluated using DMA and TGA. The  $T_{\rm g}$  of all synthesized homopolymers and copolymers were depressed relative to that of unfunctionalized VAPNB (ca. 385 °C). The extent of  $T_g$  depression was tuned by the chemical structure of the substituent and was found to follow anticipated trends with substituent size, flexibility, and types of molecular interactions. Notably, the  $T_{\rm g}$  remained at or above 150 °C for most samples, an important attribute for engineering thermoplastics. The  $T_{\rm d}$  of VAPNBs with alkyl and aryl substituents was approximately 380 °C, which is slightly depressed relative to unfunctionalized VAPNB (ca. 415 °C), In contrast, the  $T_{\rm d}$  of VAPNBs with ethereal substituents ranged from approximately 320-340 °C.

A key outcome of these studies is that VAPNB substituents have a much larger effect on  $T_{\rm g}$  than  $T_{\rm d}$ , so it is possible to broaden the service window from approximately 30 °C for unsubstituted VAPNB to 200 °C, all while maintaining a sufficiently high  $T_{\rm g}$  to maintain mechanical integrity. To further establish the viability of melt processing, a functionalized VAPNB with  $T_{\rm g}$  of 209 °C and  $T_{\rm d}$  of 376 °C was melt extruded and molded into bars at 250 °C. The bars were subjected to tensile testing, then dissolved for characterization by GPC and NMR, and finally recast for DMA testing. These post-extrusion analyses demonstrate that melt processed VAPNBs show only minor signs of degradation from processing at high temperatures under flow.

## Conflicts of interest

There are no conflicts to declare.

# Acknowledgements

This work is supported in part by the American Chemical Society Petroleum Research Fund (ACS-PRF, Award # 59132-ND7), and in part by the U.S. Department of Energy's Office of Energy Efficiency and Renewable Energy (EERE) under the award number DE-EE0009177 provided to the University of Tennessee - Oak Ridge Innovation Institute (UT-ORII). XW was supported in part by the ACS-PRF and the UT-ORII Science Alliance Graduate Advancement, Training, and Education (GATE) program. A portion of the research was conducted at the Center for Nanophase Materials Sciences (CNMS), which is a DOE Office of Science User Facility. The authors thank Yangyang Wang (Oak Ridge National Laboratory, CNMS) for assistance with DMA and MDSC experiments. WAXS experiments were enabled by the Major Research Instrumentation program of the National Science Foundation under Award No. DMR-1827474. The authors also thank Boulder Scientific for their generous donation of LiBAr<sup>F</sup><sub>4</sub>.

## References

- E. S. Finkelshtein, M. V. Bermeshev, M. L. Gringolts,
   L. Starannikova and Y. P. Yampolskii, Russ. Chem. Rev.,
   2011, 80, 341.
- 2 K. H. Park, R. J. Twieg, R. Ravikiran, L. F. Rhodes, R. A. Shick, D. Yankelevich and A. Knoesen, *Macromolecules*, 2004, 37, 5163–5178.
- 3 N. R. Grove, P. A. Kohl, S. A. Bidstrup Allen, S. Jayaraman and R. Shick, *J. Polym. Sci., Part B: Polym. Phys.*, 1999, 37, 3003–3010.
- 4 M. Chen, W. Zou, Z. Cai and C. Chen, *Polym. Chem.*, 2015, **6**, 2669–2676.
- 5 Y. Bai, P. Chiniwalla, E. Elce, R. A. Shick, J. Sperk, S. A. B. Allen and P. A. Kohl, *J. Appl. Polym. Sci.*, 2004, 91, 3023–3030.

- 6 B. L. Goodall, WO Pat, 95/14048, 1995.
- 7 B.-G. Shin, T.-Y. Cho, D. Y. Yoon and B. Liu, *Macromol. Res.*, 2007, 15, 185–190.
- 8 S. Breunig and W. Risse, *Makromol. Chem.*, 1992, **193**, 2915–2927.
- 9 W. Zhou, X. He, Y. Chen, M. Chen, L. Shi and Q. Wu, *J. Appl. Polym. Sci.*, 2011, **120**, 2008–2016.
- 10 K. R. Gmernicki, E. Hong, C. R. Maroon, S. M. Mahurin, A. P. Sokolov, T. Saito and B. K. Long, ACS Macro Lett., 2016, 5, 879–883.
- 11 D.-G. Kim, T. Takigawa, T. Kashino, O. Burtovyy, A. Bell and R. A. Register, *Chem. Mater.*, 2015, 27, 6791–6801.
- 12 S. V. Mulpuri, J. Shin, B.-G. Shin, A. Greiner and D. Y. Yoon, *Polymer*, 2011, 52, 4377–4386.
- 13 K. D. Dorkenoo, P. H. Pfromm and M. E. Rezac, *J. Polym. Sci., Part B: Polym. Phys.*, 1998, **36**, 797–803.
- 14 E. C. Kim, M.-J. Kim, L. N. Thi Ho, W. Lee, J.-W. Ka, D.-G. Kim, T. J. Shin, K. M. Huh, S. Park and Y. S. Kim, *Macromolecules*, 2021, 54, 6762–6771.
- C. R. Maroon, J. Townsend, K. R. Gmernicki,
   D. J. Harrigan, B. J. Sundell, J. A. Lawrence III,
   S. M. Mahurin, K. D. Vogiatzis and B. K. Long,
   Macromolecules, 2019, 52, 1589–1600.
- 16 S. Liu, Y. Chen, X. He, L. Chen and W. Zhou, J. Appl. Polym. Sci., 2011, 121, 1166–1175.
- 17 M. Mandal, G. Huang and P. A. Kohl, *J. Membr. Sci.*, 2019, 570, 394–402.
- 18 A. C. Kuo, *Polymer data handbook*, Oxford University Press, Inc, 1999.
- 19 E. J. Stober and J. C. Seferis, *Polym. Eng. Sci.*, 1988, **28**, 634–639.
- 20 G. Molnár, A. Botvay, L. Pöppl, K. Torkos, J. Borossay, Á. Máthé and T. Török, *Polym. Degrad. Stab.*, 2005, 89, 410–417.
- 21 G. Lisa, E. Avram, G. Paduraru, M. Irimia, N. Hurduc and N. Aelenei, *Polym. Degrad. Stab.*, 2003, 82, 73–79.
- 22 L. Perng, J. Appl. Polym. Sci., 2001, 79, 1151-1161.
- 23 A. S. Alaboodi and S. Sivasankaran, *J. Manuf. Process.*, 2018, 35, 479–491.
- 24 G. Deng, S. Hayakawa and L. F. Rhodes, *US Pat*, 20210198392, 2021.
- 25 B. L. Goodall, in *Late transition metal polymerization catalysis*, ed. L. S. B. Bernhard Rieger, S. Kacker and S. Striegler, WILEY-VCH Verlag GmbH & Co. KGaA, Weinheim, 2003, ch. 4, pp. 101–154.
- 26 W. McDougall, S. Farling, R. Shick, S. Glukh, S. Jayaraman, L. Rhodes, R. Vicari, P. Kohl, S. Bidstrup-Allen and P. Chiniwalla, Avatrel™ dielectric polymers for HDP applications, Proc. International Conference and Exhibition on High-Density Interconnect and Systems Packaging, Denver, CO, USA, 1999.
- 27 B. Goodall and D. Barnes, *Polym. Prepr. (Am. Chem. Soc., Div. Polym. Chem.)*, 1998, 39, 216–217.
- 28 B. L. Goodall, G. M. Benedikt, L. H. McIntosh III and D. A. Barnes, *US Pat*, 5468819, 1995.
- 29 B. L. Goodall, W. Risse and J. P. Mathew, *US Pat*, 5705503, 1998

30 D.-G. Kim, A. Bell and R. A. Register, ACS Macro Lett., 2015,

4, 327-330.

**Polymer Chemistry** 

- 31 S. D. Tsai and R. A. Register, Macromol. Chem. Phys., 2018, **219**, 1800059.
- 32 A. S. Abu-Surrah, U. Thewalt and B. Rieger, J. Organomet. Chem., 1999, 587, 58-66.
- 33 E. A. Lewis and B. D. Vogt, J. Polym. Sci., Part B: Polym. Phys., 2018, 56, 53-61.
- 34 J. Lipian, R. A. Mimna, J. C. Fondran, D. Yandulov, R. A. Shick, B. L. Goodall, L. F. Rhodes and J. C. Huffman, Macromolecules, 2002, 35, 8969-8977.
- 35 P. Leber, K. Kidder, D. Viray, E. Dietrich-Peterson, Y. Fang and A. Davis, J. Phys. Org. Chem., 2018, 31, e3888.
- 36 H. Koch and W. Haaf, Justus Liebigs Ann. Chem., 1960, 638, 111-121.
- 37 M. Jean and P. Van de Weghe, Tetrahedron Lett., 2011, 52, 3509-3513.
- 38 J. M. Blanco, F. Fernández, X. García-Mera and J. E. Rodríguez-Borges, Tetrahedron, 2002, 58, 8843-8849.
- 39 S. H. Kim, M. A. Worsley, C. A. Valdez, S. J. Shin, C. Dawedeit, T. Braun, T. F. Baumann, S. A. Letts, S. O. Kucheyev and K. J. J. Wu, RSC Adv., 2012, 2, 8672-8680.
- 40 T. G. Driver, A. K. Franz and K. Woerpel, J. Am. Chem. Soc., 2002, 124, 6524-6525.
- 41 K. Müller, S.-H. Chun, A. Greiner and S. Agarwal, Des. Monomers Polym., 2005, 8, 237-248.
- 42 A. Richard, Faraday Discuss., 1994, 98, 219-230.
- 43 D. A. Barnes, G. M. Benedikt, B. L. Goodall, S. S. Huang, H. A. Kalamarides, S. Lenhard, L. H. McIntosh, K. T. Selvy, R. A. Shick and L. F. Rhodes, Macromolecules, 2003, 36, 2623-2632.

- 44 D. A. Alentiev, M. V. Bermeshev, L. E. Starannikova, E. V. Bermesheva, V. P. Shantarovich, V. G. Bekeshev, Y. P. Yampolskii and E. S. Finkelshtein, J. Polym. Sci., Part A: Polym. Chem., 2018, 56, 1234-1248.
- 45 R. García-Loma and A. C. Albéniz, Asian J. Org. Chem., 2019, 8, 304-315.
- 46 A. D. Hennis, J. D. Polley, G. S. Long, A. Sen, D. Yandulov, J. Lipian, G. M. Benedikt, L. F. Rhodes and J. Huffman, Organometallics, 2001, 20, 2802-2812.
- 47 S. Kim, S. Hewlett, C. Roth and J. M. Torkelson, Eur. Phys. J. E: Soft Matter Biol. Phys., 2009, 30, 83.
- 48 P. Gill, S. Sauerbrunn and M. Reading, J. Therm. Anal., 1993, 40, 931-939.
- 49 G. Odian, Principles of polymerization, John Wiley & Sons, 4th edn., 2004.
- 50 P. Patel, T. R. Hull, R. W. McCabe, D. Flath, J. Grasmeder and M. Percy, Polym. Degrad. Stab., 2010, 95, 709-718.
- 51 E. Penzel, J. Rieger and H. Schneider, Polymer, 1997, 38, 325-337.
- 52 M. Gordon and J. S. Taylor, J. Appl. Chem., 1952, 2, 493-500.
- 53 K. Müller, S. Kreiling, K. Dehnicke, J. Allgaier, D. Richter, L. J. Fetters, Y. Jung, D. Y. Yoon and A. Greiner, Macromol. Chem. Phys., 2006, 207, 193-200.
- 54 H. Stretz and D. Paul, *Polymer*, 2006, 47, 8527–8535.
- 55 L. F. Rhodes, R. Vicari, L. J. Langsdorf, A. A. Sobek, E. P. Boyd and B. Bennett, WO Pat, 2003050158A1, 2003.
- 56 D. C. Lee, V. K. Kensy, C. R. Maroon, B. K. Long and A. J. Boydston, Angew. Chem., 2019, 131, 5695-5698.
- 57 H. Hinsken, S. Moss, J.-R. Pauquet and H. Zweifel, Polym. Degrad. Stab., 1991, 34, 279-293.